Subbands and Landau levels in the two-dimensional hole gas at the GaAs-$Al_xGa_{1-x}As$ interface

U. Ekenberg and M. Altarelli
Max-Planck-Institut für Festkörperforschung, Heisenbergstrasse 1, D-7000 Stuttgart 80, Federal Republic of Germany
(Received 29 April 1985)

The hole subbands and Landau levels in the inversion layer at the interface between GaAs and *p*-type $Al_xGa_{1-x}As$ are calculated self-consistently in the Hartree approximation. The degenerate valence-band structure and the matching of the wave function at the interface are taken into account. Without magnetic field we calculate the subband dispersion parallel to the interface. The subbands are found to be strongly nonparabolic and spin split. The calculated classical cyclotron effective masses do not agree very well with those found in cyclotron resonance experiments. We have therefore included the magnetic field in the calculation. The B dependence of the Landau levels is found to be strongly nonlinear. The calculated transition energies are partly in very good agreement with experiment. The dependence of the results on areal hole density, doping concentrations, valence-band discontinuity, etc., is also investigated.

I. INTRODUCTION

Recently there has been an increasing experimental interest in the properties of the two-dimensional (2D) hole gas formed at the interface between nominally undoped GaAs and *p*-type $Al_xGa_{1-x}As$.[1-5] The integral[3] and fractional[2] quantized Hall effects have been observed in this structure, and it has been demonstrated that the comparatively high hole mobility can be utilized in a transistor.[6,7] Very recently it has been shown that the 2D hole gas can be utilized in a new type of complementary transistor structure.[8] In a recent paper[9] we showed that the degeneracy of the valence band leads to unexpected features of the subband dispersion parallel to the surface. In that paper we used the Luttinger Hamiltonian[10,11] in the spherical approximation.[12] In this paper we have gone further and used an approximation that should be better for the (001) interface, which is usually studied experimentally.

The experiments with which our results can be compared are often carried out in magnetic fields. We show that it is important to include the magnetic field in the calculation to obtain good agreement with experiment. Because the $E(k_{\|})$ dispersion is nonparabolic, the B dependence of the Landau levels is nonlinear and the anticrossing behavior between the levels leads to a quite peculiar B dependence. The Landau-level structure can no longer be described in terms of one effective mass per subband, and the effective masses turn out to be dependent on the magnetic field. Our results are in quite good agreement with experimentally determined cyclotron resonance effective masses.

This problem has recently been treated theoretically by other authors[13,14] who have used similar methods but obtained less good agreement with experiment. We discuss the differences between the calculations and propose explanations for the discrepancies. In Sec. II A we outline the theory which we use to calculate the subband dispersion without magnetic field, and in Sec. II B we describe the modifications done when the magnetic field is nonzero. The results are presented in Sec. III and discussed in Sec. IV. Finally, Sec. V contains the conclusions.

II. THEORY

A. Without magnetic field

In order to calculate the hole subbands one must take the degeneracy of the valence band into account. We neglect the splitoff band, which in GaAs is 0.34 eV below the valence-band edge;[15] this consists of the heavy-hole band and the light-hole band, which are degenerate at $k=0$ in the bulk. Each of these bands has a twofold spin degeneracy if we have inversion symmetry. These two bands can be described by a 4×4 matrix with three valence-band parameters γ_1, γ_2, and γ_3, which correspond to inverse effective masses.[10] This matrix was written by Baldereschi and Lipari[12] with the use of second-rank irreducible tensor operators in a way that clearly expresses the symmetry of the different terms and that is convenient for calculation of acceptor levels

$$H=E_v-\frac{\gamma_1}{2m_0}p^2+\frac{2\gamma_2+3\gamma_3}{45m_0}(P^{(2)}\cdot J^{(2)})-\frac{\gamma_3-\gamma_2}{18m_0}\times\left\{[P^{(2)}\times J^{(2)}]^{(4)}_{-4}+\frac{\sqrt{70}}{5}[P^{(2)}\times J^{(2)}]^{(4)}_{0}+[P^{(2)}\times J^{(2)}]^{(4)}_{4}\right\}. \quad (1)$$

Here the J's are 4×4 matrices, which represent spin-$\frac{3}{2}$ operators. In one convenient representation the matrix can be written

$$H=E_vI+\frac{\hbar^2}{2m_0}\begin{bmatrix} A_+ & B & C & 0 \\ B^* & A_- & 0 & C \\ C^* & 0 & A_- & -B \\ 0 & C^* & -B^* & A_+ \end{bmatrix}, \quad (2)$$

where

$$A_{\pm}=-(\gamma_1\pm\gamma_2)(k_x^2+k_y^2)-(\gamma_1\mp 2\gamma_2)k_z^2\ , \tag{3}$$

$$B=2\sqrt{3}\gamma_3(\{k_z,k_x\}-i\{k_y,k_z\})\ , \tag{4}$$

and

$$C=\sqrt{3}[\gamma_2(k_x^2-k_y^2)-2i\gamma_3\{k_x,k_y\}]\ . \tag{5}$$

Here I is the unit matrix and $\{\ ,\ \}$ denotes the anticommutator. (With a magnetic field included the different k components do not in general commute.) We neglect the linear terms in the Hamiltonian caused by the violation of inversion symmetry in the bulk[16] because it has been shown that these give quite a small effect.[14] In our previous paper we used the spherical approximation,[12] i.e., in Eq. (1) we only included the first three terms, which have spherical symmetry. This corresponds to replacing γ_2 and γ_3 by $\bar{\gamma}=(2\gamma_2+3\gamma_3)/5$ everywhere in Eq. (2). For a (001) interface it is not much more complicated to use the axial approximation, which was introduced by Lipari and Altarelli[17] for the calculation of indirect excitons. Then the middle term in large parentheses in Eq. (1) is also retained and the Hamiltonian becomes cylindrically symmetric. In the matrix (2) this turns out to imply the replacement of γ_2 and γ_3 in the term C [Eq. (5)] by $\tilde{\gamma}=(\gamma_2+\gamma_3)/2$. This approximation implies that the anisotropy in the xy plane is neglected. This is convenient in the self-consistent part of the calculation, where the circular symmetry of the Fermi surface leads to important simplifications.

We choose the z direction to be perpendicular to the (001) interface between the semi-infinite GaAs layer ($z<0$) and the semi-infinite $Al_xGa_{1-x}As$ layer ($z>0$). In Eq. (2) we replace k_z by $-i(d/dz)$, and along the diagonal we add the potential $V(z)$, which is shown in a typical case in Fig. 1. $V(z)$ consists of two parts, the potential due to the 2D hole gas in the inversion layer in GaAs, $V^{\rm inv}$, and the potential due to the ionized impurities in the depletion layers, $V^{\rm dep}$.

$V^{\rm inv}$ is calculated self-consistently in the Hartree approximation by solving Poisson's equation numerically. The calculations are done for $T=0$. Many-body effects such as exchange and correlation for a two-dimensional hole gas have been treated using a simplified valence-band structure by Ohkawa[18] for the case of a Si-SiO_2 interface. Such effects remain to be investigated in the present case. $V^{\rm dep}$ is treated in the depletion-layer approximation, i.e., all donors in the GaAs are assumed to be ionized for $-l_n<z<0$ ($l_n>0$) and, similarly, all acceptors in the $Al_xGa_{1-x}As$ for $0<z<l_p$. In order to obtain high carrier mobilities a thin undoped $Al_xGa_{1-x}As$ layer (spacer layer) of thickness d is often inserted between the undoped GaAs layer and the doped $Al_xGa_{1-x}As$ layer. The effect on the band bending of this spacer layer can easily be taken into account. In this case the depletion-layer widths l_n and l_p are obtained from the equations

$$l_nN_d+N_s=l_pN_a \tag{6}$$

and

$$V_p(d+l_p)+V_n(-l_n)=E_g(\mathrm{GaAs})+\Delta E_v-\delta_1-\delta_2\ , \tag{7}$$

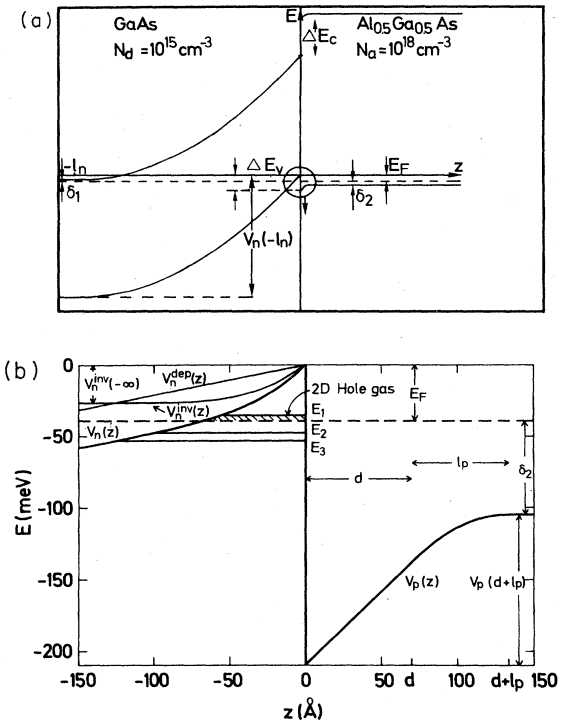

FIG. 1. Band diagram for the (001) GaAs-$Al_{0.5}Ga_{0.5}As$ interface. A portion of (a) is magnified in (b), where the calculated energy levels at $k_{||}=0$ and the potentials V_n in GaAs and V_p in $Al_{0.5}Ga_{0.5}As$ are drawn. We have also separately drawn the contributions from the holes in the inversion layer $V_n^{\rm inv}$ and from the depletion layer $V_n^{\rm dep}$ to the total potential V_n in GaAs.

where[19]

$$V_n(-l_n)=\frac{2\pi e^2}{\epsilon_1}N_dl_n^2+V^{\rm inv}(-\infty) \tag{8}$$

and

$$V_p(d+l_p)=\frac{2\pi e^2}{\epsilon_2}N_al_p^2+\frac{4\pi e^2}{\epsilon_2}N_al_pd\ . \tag{9}$$

Here δ_1 and δ_2 are the Fermi levels in the GaAs and $Al_xGa_{1-x}As$ relative to the nearest band edge, respectively (see Fig. 1), and ϵ_1 and ϵ_2 are the corresponding dielectric constants. The valence-band discontinuity at the interface is denoted by ΔE_v, the acceptor concentration in the $Al_xGa_{1-x}As$ by N_a, the donor concentration in GaAs by N_d, and the areal hole density in the inversion layer by N_s. [If the GaAs is compensated, N_d should be replaced by $N_d(\mathrm{GaAs})-N_a(\mathrm{GaAs})$ and similarly for the $Al_xGa_{1-x}As$.]

Equation (6) comes from the charge-neutrality requirement while Eq. (7) comes from the requirement that the Fermi level should be constant and can be verified from inspection of Fig. 1. After each iteration in the calculation of $V^{\rm inv}$ new values of l_n and l_p are determined.

Since the dielectric constants of GaAs and $Al_xGa_{1-x}As$ are slightly different, one should in principle also include the image potential. In the commonly used

form it has a singularity at the interface. Stern and Das Sarma[20] have pointed out that this singularity is unphysical and have done calculations for the 2D electron gas for the more realistic case with a continuously but rapidly varying dielectric constant. In this case they found that the effect of the image potential is quite small and for this reason we have neglected it in the present paper.

The matching of the wave function at the interface is taken into account using a modified variational method[21] described in more detail earlier.[22] Instead of just finding the eigenvalues of the Hamiltonian matrix, we find the eigenvalues of a matrix with the following structure:

$$\begin{bmatrix} H_A+I_{AA} & I_{AB} \\ I_{BA} & H_B+I_{BB} \end{bmatrix} . \tag{10}$$

H_A and H_B are the usual Hamiltonian matrices [Eq. (2)] with the γ's and E_v for material A (GaAs) and B ($Al_xGa_{1-x}As$) inserted. The "interface functionals" $I_{\alpha\beta}$ assure that the boundary conditions are fulfilled.

The envelope function is expanded in basis functions of two types:

$$\Phi_i = N \exp[-b_i(z-a_i)^2] \tag{11}$$

and

$$\Phi_i' = N'(z-a_i)\exp[-b_i(z-a_i)^2] . \tag{12}$$

We have found that the convergence becomes good for six suitably chosen pairs of the adjustable parameters (a_i,b_i). In the general case we obtain a 96×96 matrix, which is diagonalized numerically for each value of $k_{||}$, the wave vector parallel to the interface.

After the calculation of the subbands we have determined the classical cyclotron effective masses defined by

$$m^* = \frac{\hbar^2}{2\pi}\frac{dA(E)}{dE}\bigg|_{E=E_F} , \tag{13}$$

where $A(E)$ is the area in the $k_{||}$ plane with constant energy E. As mentioned earlier, we have taken the self-consistent potential $V(z)$ from the axial model, in which this constant energy contour is a circle. In this case Eq. (13) simplifies further to

$$m^* = \hbar^2 k \left[\frac{dE}{dk}\right]^{-1}\bigg|_{k=k_F} . \tag{14}$$

B. With magnetic field

Many investigations of 2D electron and hole gases are carried out in magnetic fields. For the simple case with one nondegenerate parabolic conduction band the measured cyclotron effective mass coincides with that obtained from the curvature in the $E(k)$ dispersion at the band minimum. For the 2D hole gas we have found that the subband dispersion in the absence of a magnetic field is far from parabolic, and one can therefore suspect that the results in a magnetic field can also be complicated. This has, in fact, been seen in similar calculations for the GaAs-$Al_xGa_{1-x}As$ superlattice.[23] The magnetic field leads to a quantization of the orbits in the plane perpendicular to the magnetic field B, which we assume to be perpendicular to the (001) interface.

To include the magnetic field we make the following modifications to the Hamiltonian: (1) $\mathbf{k}$ is replaced by $\mathbf{k}+e\mathbf{A}/c\hbar$, where $\mathbf{A}$ is the vector potential, and (2) a term proportional to the magnetic field is added along the diagonal with the weight κ. Luttinger[10] also derived a term proportional to the parameter q, but this term is small and we therefore neglect it. The corresponding changes are made in the interface functional. In the Hamiltonian matrix, k_x and k_y are now replaced by harmonic-oscillator operators obeying the usual commutation rules. If we apply the axial approximation we find by inspection that the column vector

$$\begin{bmatrix} c_1(z)\phi_{n-1} \\ c_2(z)\phi_n \\ c_3(z)\phi_{n+1} \\ c_4(z)\phi_{n+2} \end{bmatrix} \tag{15}$$

TABLE I. Parameters used in the calculation.

	GaAs	AlAs
Valence-band parameters		
γ_1	6.85[a]	3.45[b]
γ_2	2.1[a]	0.68[b]
γ_3	2.9[a]	1.29[b]
κ	1.2[a]	0.12[c]
Dielectric constants	$\epsilon_1=12.56$[d]	$\epsilon_2=9.56$[e]
Distances between the Fermi levels and the nearest band edge [see Fig. 1(a)]	$\delta_1=6$ meV[d]	$\delta_2=35$ meV[f]

[a]Reference 26.
[b]Reference 27. Linear interpolation is used for $Al_xGa_{1-x}As$.
[c]Reference 28.
[d]Reference 29.
[e]Assuming that the variation with x at room temperature $\epsilon(Al_xGa_{1-x}As) = \epsilon(GaAs)-3.0x$ given in Ref. 30, p. 219, also holds at $T=0$.
[f]Reference 1.

becomes an eigenvector, and if we let the raising and lowering operators operate on the harmonic-oscillator functions ϕ_i of this eigenvector, the Hamiltonian matrix becomes

$$H = E_v I + \frac{\hbar^2}{2m_0} H' , \tag{16}$$

where H' is given by

$$\begin{bmatrix}
-(\gamma_1-2\gamma_2)k_z^2 - [(\gamma_1+\gamma_2)(2n-1)+3\kappa]s & 2\sqrt{6ns}\,\gamma_3 k_z & 2\sqrt{3n(n+1)}s\tilde{\gamma} & 0 \\
2\sqrt{6ns}\,\gamma_3 k_z & -(\gamma_1+2\gamma_2)k_z^2 - [(\gamma_1-\gamma_2)(2n+1)+\kappa]s & 0 & 2\sqrt{3(n+2)(n+1)}s\tilde{\gamma} \\
2\sqrt{3n(n+1)}s\tilde{\gamma} & 0 & -(\gamma_1+2\gamma_2)k_z^2 - [(\gamma_1-\gamma_2)(2n+3)-\kappa]s & -2\sqrt{6(n+2)s}\,\gamma_3 k_z \\
0 & 2\sqrt{3(n+2)(n+1)}s\tilde{\gamma} & -2\sqrt{6(n+2)s}\,\gamma_3 k_z & -(\gamma_1-2\gamma_2)k_z^2 - [(\gamma_1+\gamma_2)(2n+5)-3\kappa]s
\end{bmatrix} \tag{17}$$

Here

$$s = \frac{2eBm_0}{c\hbar} . \tag{18}$$

We have two heavy-hole and two light-hole solutions at $B=0$ for each n value if $n \geq 1$. But for $n \leq 0$ some of the coefficients $c_i(z)$ must be set equal to zero and we have fewer solutions. For the ground state, which is a heavy-hole state, we only have one Landau level for $n=-2$, -1, and 0.

We then calculate the cyclotron masses from the allowed transition energies using the definition:

$$m^* = \frac{e\hbar B}{c\Delta E} , \tag{19}$$

where ΔE is the energy difference between the two Landau levels. Two conditions must be fulfilled for a transition to take place.

(1) The selection rules must be fulfilled. They were worked out by Suzuki and Hensel[24] and by Trebin, Rössler, and Ranvaud.[25] In our case we find that we must have $\Delta n = \pm m$, where m is an odd integer. The transitions with $m=1$ are expected to be strong, while the transition probability for $m \geq 3$ comes in with the coefficient $(\gamma_3-\gamma_2)$ and would be absent if the axial approximation were exact. Transitions with $m=3$ and 5 can possibly be seen, while those with $m \geq 7$ are expected to be difficult to detect experimentally.

(2) The transitions must also take place from a filled level to an empty level. (One of these levels can be partially filled.) The filling factor ν (the number of occupied Landau levels) is given by

$$\nu = \frac{hcN_s}{eB} . \tag{20}$$

In the present case $N_s = 5\times10^{11}$ cm^{-2}, and we then find $\nu = 20.68/B$, where B is measured in T. The third level is, e.g., partially filled between $B=6.89$ and 10.34 T.

The levels can be ordered in two series, one starting with $n=-2$ and the other one starting with $n=1$. Transitions between these two series are in principle possible, but it turns out that no such transitions with $\Delta n = \pm 1$ have reasonably small transition energies, i.e., reasonably large effective masses. It should be noted that in the present case one can hardly define one effective mass corresponding to each subband for $B=0$. Instead, different transitions are possible in different B intervals, and for each transition one can define one effective mass, which in general is B dependent.

III. RESULTS

The results of the calculations depend on a number of input parameters, some of which are given in Table I. The doped material is usually assumed to consist of $Al_{0.5}Ga_{0.5}As$. Some parameters depend on the experimental conditions and can in some cases be difficult to determine experimentally. For this reason we have performed calculations for different values of the valence-band discontinuity ΔE_v, the background donor concentration in the GaAs N_d, the acceptor concentration in the $Al_xGa_{1-x}As$ N_a, and the areal hole density N_s. The band-gap difference between GaAs and $Al_xGa_{1-x}As$ is fairly well known,[30] but the question of how it is divided between the valence band and the conduction band has recently been subject to discussion. Different experimental determinations of the fraction of the band-gap discontinuity in the valence band have given quite different results, e.g., 15% (Ref. 31), 12% (Ref. 32), 43% (Ref. 33), 35% (Ref. 34), 40% (Ref. 35), and 20% (Ref. 36). In our previous paper we pointed out that the band bending in the $Al_xGa_{1-x}As$ in the heterostructure investigated by

Störmer *et al.*,[3] which had a spacer layer with $d=70$ Å, ought to be larger than ΔE_v (using Dingle's rule[31]) and we would not have any 2D hole gas in that case. Wang *et al.*[37] have used essentially the same approach to determine a new value $\Delta E_v=210$ meV for the GaAs-$Al_{0.5}Ga_{0.5}As$ interface. This is about 33% of the band-gap discontinuity according to Ref. 30. This value lies roughly in the middle of the suggested values and is supported by very recent experiments.[38] It will be used in most of the calculations.

In the paper in which the first observation of the 2D hole gas was reported, Störmer and Tsang[1] estimated that the GaAs had a net donor concentration of 10^{15} cm^{-3}. We use this value in most of our calculations. In some subsequent papers, with which we compare our results, the background doping concentration was not given and therefore we have also performed some calculations for lower donor concentrations. Unless anything else is specified, we assume that $N_a=10^{18}$ cm^{-3}, that the areal hole density in the inversion layer is $N_s=5\times10^{11}$ cm^{-2}, and that the spacer-layer width d is zero. Below we will investigate the effect when one parameter at a time is varied.

In Fig. 2 we give the subband dispersions (for $B=0$) in the spherical model[12] and in the axial model.[17] It is seen that the same general features as were pointed out in our previous paper[9,39] remain as we change from the spherical to the axial model: The subbands are split for $k\neq0$ (we will call each of these "spin subbands"), they are strongly nonparabolic, and the second subband pair even bends up close to $k=0$. The main difference is that the subbands are shifted in energy, but it is also seen that the dispersion is changed. This has a clear effect on the classical effective masses, which are given in Table II. The calculation in the axial model with the parameters given below Fig. 2 will be considered as reference results in the rest of the paper.

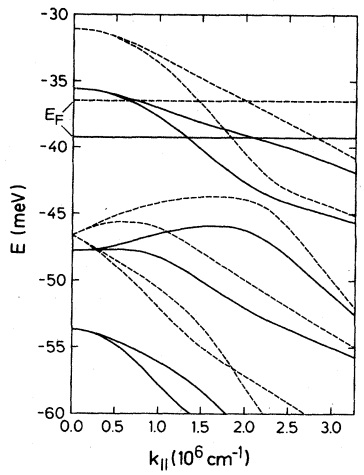

FIG. 2. Energy bands as a function of the wave vector parallel to the (001) GaAs-$Al_{0.5}Ga_{0.5}As$ interface, $k_{||}$, in the axial (solid lines) and the spherical (dashed lines) approximations. The Fermi level is drawn for each case. $N_s=5\times10^{11}$ cm^{-2}, $N_a=10^{18}$ cm^{-3}, $N_d=10^{15}$ cm^{-3}, $\Delta E_v=210$ meV, $d=0$.

TABLE II. Classical effective masses for the GaAs-$Al_{0.5}Ga_{0.5}As$ interface for different input parameters and different models. The results in the first row are for the axial model and the following parameters: $N_s=5\times10^{11}$ cm^{-2}, $N_a=10^{18}$ cm^{-3}, $N_d=10^{15}$ cm^{-3}, $\Delta E_v=210$ meV, and $d=0$. m_+^* and m_-^* denote the higher and the lower masses corresponding to the upper and the lower filled spin subbands in Fig. 2.

Parameter changes	m_+^*	m_-^*
None	0.890	0.198
$\Delta E_v=94$ meV[a]	0.981	0.271
125 meV[b]	0.943	0.231
269 meV[c]	0.878	0.190
2000 meV	0.818	0.165
$N_d=10^{14}$ cm^{-3}	0.873	0.195
10^{13} cm^{-3}	0.827	0.196
$N_a=2\times10^{18}$ cm^{-3}	0.852	0.200
$\gamma_1=6.98$, $\gamma_2=2.25$, $\gamma_3=2.88$[d]	0.758	0.190
Spherical approximation	0.479	0.162
Exact Hamiltonian	0.990	0.196
Experiment[e]	0.60	0.38

[a] ΔE_v taken from Ref. 31.
[b] Reference 36.
[c] Reference 33.
[d] Valence-band parameters for GaAs taken from Ref. 40.
[e] Reference 3.

Using the self-consistent potential from the axial-model calculation fixed we have also calculated the subband dispersion using the exact valence-band Hamiltonian (2) for k values in different directions in the k_x-k_y plane. In Fig. 3 we give the dispersions in the [100] and [110] directions and compare them with the result in the axial model, which, as expected, lies in between these results. In Fig. 4 we have shown the Fermi surfaces for the upper-

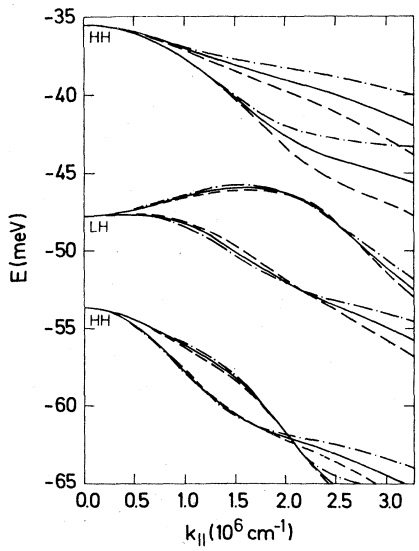

FIG. 3. Energy bands as a function of $k_{||}$, for the GaAs-$Al_{0.5}Ga_{0.5}As$ interface in the [100] direction (dashed lines), in the [110] direction (dot-dashed lines), and according to the axial approximation (solid lines). N_s, N_a, N_d, ΔE_v, and d are the same as in Fig. 2.

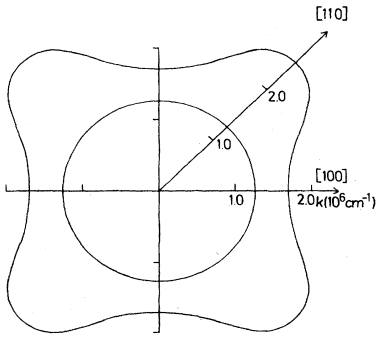

FIG. 4. Fermi surfaces for the uppermost subband pair for wave vectors parallel to the GaAs-$Al_{0.5}Ga_{0.5}As$ interface. The parameters are the same as in Fig. 2.

most subband pair. It is seen that the Fermi surface of the spin subband corresponding to the higher effective mass is strongly anisotropic, while the other one is almost isotropic. However, it should be noted that also for the latter spin subband there is a clear difference between the dispersions in the different directions for wave vectors larger than the Fermi wave vector, as is seen in Fig. 3. We have found that about 72% of the charge is in the uppermost spin subband. This value is higher than the experimental result, 61%.[3] The better agreement in our previous calculation[9] was accidental and due to the use of the less-accurate spherical approximation.

We have also performed calculations for other values of ΔE_v, including $\Delta E_v = 2$ eV, in order to compare with other calculations where an infinite ΔE_v value was assumed. When ΔE_v is varied, it is found that the light-hole bands are shifted more than the heavy-hole bands. We have also found that the effective masses are changed. As is seen in Table II the lower mass changes almost by a factor of 2 as we go from $\Delta E_v = 94$ meV ($=0.15\Delta E_g$) to $\Delta E_v = 2$ eV. In the latter case we have also found that the inner Fermi surface becomes almost exactly a circle and that the outer circle becomes less warped than in Fig. 4, in qualitative agreement with other calculations.[13,14]

The background doping concentration in the GaAs is of course difficult to measure accurately, but we have found that it influences the results, in particular the intersubband separations, significantly. A similar conclusion was drawn by Stern and Das Sarma[20] for the interface between GaAs and n-type $Al_xGa_{1-x}As$. From Eqs. (6)—(9) one sees that a decrease in N_d leads to a smaller slope of $V_n^{\rm dep}$ in Fig. 1 and that the total potential thus becomes wider. Our calculations indicate that the total band bending due to the inversion layer potential $V^{\rm inv}(-\infty)$ simultaneously increases somewhat. The total effect is that the absolute values of the subband energies decrease and the effective masses are also affected. We will tell more about this effect when we come to the case with $B \neq 0$.

The quantities N_a, N_s, and d are clearly interrelated. We have, however, found that the dependence of the subband dispersion on the spacer-layer width d is negligible as long as d is in the experimentally interesting range. For this reason we can vary N_a or N_s separately within certain limits, assuming that one of these parameters is kept fixed by a suitable change of d. If we set $d = 70$ Å to obtain the same structure as in Ref. 3, and compare the band bending in the $Al_xGa_{1-x}As$ to ΔE_v and E_F in the inversion layer, we find that our results are consistent with a value of $\delta_2 = 66$ meV. The Fermi level in the bulk $Al_xGa_{1-x}As$ would be at the acceptor level if it were lightly p doped and compensated. However, δ_2 is fairly uncertain in the present case due to the heavy doping of the $Al_xGa_{1-x}As$. As an input parameter, δ_2 is only used in Eq. (7), where the right-hand side is clearly dominated by E_g.

As is seen in Table II the classical effective masses do not agree very well with those found experimentally by Störmer *et al.*,[3] 0.60 and 0.38 (in units of the free-electron mass). The agreement becomes much better if we include the magnetic field in the calculation and compute the Landau levels. These are shown in Fig. 5 for the "reference material" (same parameters as in Fig. 2). As was mentioned above the calculations with a magnetic field are done in the axial approximation. If the subband dispersion were parabolic one could expect the Landau levels to vary linearly with the magnetic field. We see, however, that the dependence is far from linear and that many of them tend to become horizontal for large magnetic fields. This is due to the repulsion between the levels belonging to the first subband pair and those of the second pair having the same Landau-level index.

To compare with the experimental results we have calculated the energies for transitions obeying the selection rule $\Delta n = \pm 1$ between Landau levels of which one is (partially) filled and one is (partially) empty. In Fig. 6 we have also included the experimental results from Ref. 3.

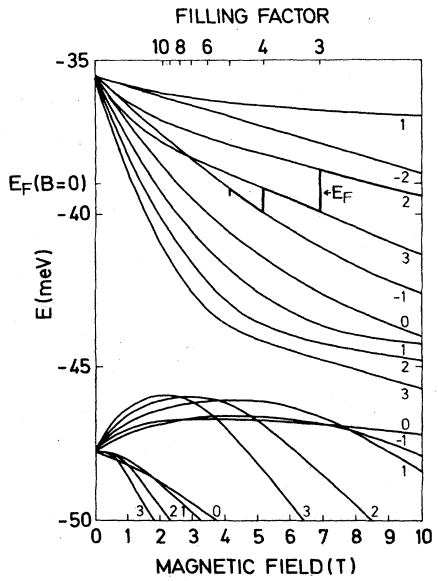

FIG. 5. Landau levels with indices ≤ 3 (shown at each line) as a function of the magnetic field in the hole gas at the GaAs-$Al_{0.5}Ga_{0.5}As$ interface. The filling factor ν [Eq. (20)] is given at the top of the figure. The thick line indicates the position of the Fermi level for high magnetic fields. Same parameters as in Fig. 2.

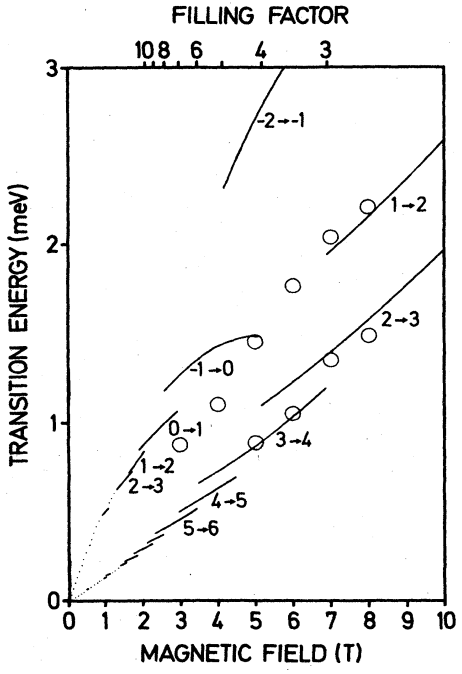

FIG. 6. Calculated transition energies, i.e., Landau-level separations for transitions obeying the selection rule $\Delta n = \pm 1$ and the occupation requirements (see text), as a function of magnetic field for the GaAs-$Al_{0.5}Ga_{0.5}As$ interface (solid lines). The indices of the Landau levels between which the transitions take place are indicated near the lines. The dots for small B values are interpolated values. The open circles are the experimental results by Störmer *et al.* (Ref. 3). Same parameters as in Fig. 2.

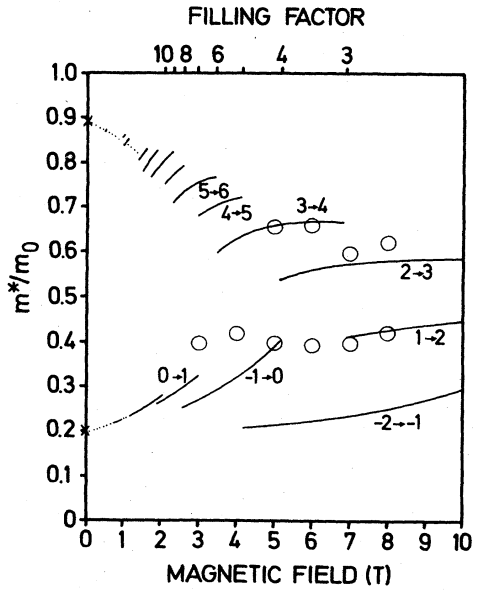

FIG. 7. Effective masses (in units of the free-electron mass m_0) calculated using Eq. (19) for the transitions shown in Fig. 6 (solid lines). The indices for the Landau levels involved in the transitions are indicated. The crosses for $B = 0$ are the classical effective masses in the axial approximation calculated with the use of Eq. (14). The dots are interpolated values. The open circles are the experimental results from Ref. 3. Same parameters as in Fig. 2.

It should be noted that the transitions to an almost-full level or from an almost-empty level should be weak, but for most magnetic fields one should expect to see three strong transitions. These transitions all have $\Delta n = +1$ and should be seen together with those with $\Delta n = -3$ and $\Delta n = +5$ (weak transitions) for incident light with one circular polarization. The transitions with $\Delta n = -1$ are all found to have quite high transition energies. Therefore, we predict that the spectrum with the opposite circular polarization should be fairly structureless at not-too-high energies. For each of the transitions shown in Fig. 6 we have also calculated the corresponding effective mass using Eq. (19) and have shown the results in Fig. 7. It is clear that the effective mass depends on the magnetic field for two reasons: (1) The energy difference between two given Landau levels varies with magnetic field in a nonlinear way and (2) transitions between different pairs of Landau levels become possible in different B ranges depending on the position of the Fermi level.

The agreement with experiment for the higher mass is very good. The trend that it increases with decreasing magnetic field and approaches the classical effective mass in the limit $B \to 0$ is also clear. The two experimental points in Fig. 6 for the highest B values are not quite along the same straight line as the two points for lower B values and we suggest that this is a real effect caused by the change of allowed transitions with magnetic field. We have found in our calculations that these transition energies are not very sensitive to the input parameters.

The lower mass is also in quite good agreement with experiment for $B \geq 7$ T, where it corresponds to a transition between levels with Landau-level indices 1 and 2. Between 5.1 and 6.9 T, where both these levels are filled, we have found no effective masses in agreement with the experimental value 0.38. One possible reason for this disagreement is that we have used the axial approximation in the Landau-level calculation. If the exact Hamiltonian is used, Landau levels with n and $n \pm 4$ are coupled.[41] This implies in particular that the Landau levels with $n = -1$ and 3 in Fig. 5 should not cross and that these two levels actually have mixed $n = -1$ and 3 characters. At still lower magnetic fields we again have some transitions with energies in reasonable agreement with experiment. It should be noted that these levels are quite sensitive to the input parameters in the calculation. The trend is clear, however, that the lower mass decreases with decreasing B, in contrast to the heavier mass.

This is in good agreement with the recent experimental results by Eisenstein *et al.*,[5] where effective masses in the region 0.25–0.3 were obtained for low magnetic fields. This sample differed from that in Ref. 3 mainly in that N_a was 2×10^{18} cm^{-3} instead of 10^{18} cm^{-3}. We have performed calculations for the parameters of x, N_s, N_a, and d used in Ref. 5, for $N_d = 10^{15}$ cm^{-3} and for different values of ΔE_v. The calculated lower effective masses for $B = 1$ T are shown in Table III together with the experimental result. For $\Delta E_v = 90$ meV, i.e., the "old" value according to Ref. 31, the agreement is quite good. In this case we have also found that the effective mass is 0.273 at $B = 0.5$ T and that 70% of the charge is in the uppermost

TABLE III. Lower cyclotron effective mass (m^*_-) at $B=1$ T for the GaAs-$Al_{0.48}Ga_{0.52}As$ interface for different values of ΔE_v. $N_s=4.8\times10^{11}$ cm^{-2}, $N_a=2\times10^{18}$ cm^{-3}, $N_d=10^{15}$ cm^{-3}, $d=0$.[a]

ΔE_v (meV)	m^{*b}_-
90[c]	0.306
120[d]	0.266
201[e]	0.227
258[f]	0.222, 0.220
Experiment[g]	0.30

[a]The sample actually had a spacer layer of width $d=140$ Å. For small values of ΔE_v this would lead to the situation when no 2D hole gas can be formed. We have ensured that for $\Delta E_v=258$ meV the difference between the results for $d=0$ and 140 Å is negligible.

[b]As is seen in Figs. 6 and 7 and discussed in the text, we have in general two m^*_+ values and one m^*_- value or one m^*_+ value and two m^*_- values, depending on the position of the Fermi level.

[c]ΔE_v taken from Ref. 31.

[d]Reference 36.

[e]Reference 37 (or 38).

[f]Reference 33.

[g]Extrapolated value from Ref. 5.

spin subband (for $B=0$). Both results agree very well with experiment. This should not be taken as an attempt to determine ΔE_v. The effective masses also depend on other factors.

If we vary different input parameters, we find that the effective masses are fairly insensitive to the acceptor concentration in the $Al_xGa_{1-x}As$, N_a. A change in the background donor concentration in the GaAs, N_d, has a clear effect on some transition energies while other transition energies are almost unaffected, e.g., the transition considered in Table III. If we change the hole density N_s, keeping the other parameters fixed, we can see in Fig. 8 that the cyclotron effective masses at $B=5$ T for each transition depend only weakly on N_s but that the effective masses change considerably because different transitions are possible in different ranges of N_s since the filling factor ν changes. For comparison we have also shown the classical effective masses (for $B=0$) calculated according

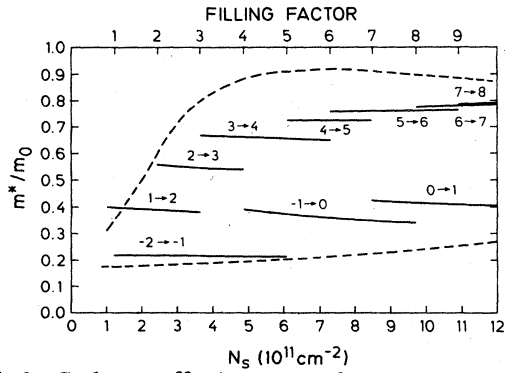

FIG. 8. Cyclotron effective masses for $B=5$ T (solid lines) and classical effective masses for $B=0$ T (dashed lines) as a function of the areal hole density N_s in the inversion layer at the GaAs-$Al_{0.5}Ga_{0.5}As$ interface. The indices for the Landau levels involved in each transition are indicated. N_a, N_d, ΔE_v, and d are the same as in Fig. 2.

to Eq. (14). They are fairly constant except for a sharp rise of the higher mass up to $N_s=4\times10^{11}$ cm^{-2}. We have also noted that the subbands at $k=0$ do not follow an $N_s^{2/3}$ dependence as is sometimes assumed. We rather find that $E(0)$ varies as N_s^α with $0.2\leq\alpha\leq0.5$, where α is different for different subbands and different N_s ranges. For $N_s=1.2\times10^{12}$ cm^{-2} the band bending (for $d=0$) in the $Al_xGa_{1-x}As$ is so large that the Fermi level in the bulk would be just above the valence-band edge instead of a distance δ_2 above it. Thus we can conclude that for $N_a=10^{18}$ cm^{-3} and $N_d=10^{15}$ cm^{-3} one cannot reach higher hole densities than about 10^{12} cm^{-2} (unless a gate voltage is applied). Even for the highest N_s value considered we are far from the situation when the second subband starts to get filled. To reach this situation much heavier doping of the $Al_xGa_{1-x}As$ is needed.

IV. DISCUSSION

We have seen that for quantitative calculations for two-dimensional hole systems one cannot describe the valence band in terms of a few effective masses but must take the degeneracy into account. We have made some approximations of which the most important one probably is the neglect of many-body effects. Such effects have been considered for n-channel inversion layers at the $Si-SiO_2$ interface[42] and more recently for the GaAs-$Al_xGa_{1-x}As$ interface.[43,20] Ando[42,43] concluded that they are important in the former case but less important in the latter case. For p-channel Si inversion layers the experimentally determined effective masses differ by a factor of 2 between two different research groups. Landwehr *et al.*[44] found good agreement between one set of data and calculations of the classical cyclotron mass in the Hartree approximation. It should be noted that N_s was fairly high (10^{12}–10^{13} cm^{-2}) in these experiments. On the other hand, Ohkawa[18] has calculated the many-body enhancements of the effective hole masses in a p-channel Si inversion layer and found them to be substantial for the comparatively small areal hole density considered in the present paper. We have found quite good agreement for the GaAs-$Al_xGa_{1-x}As$ interface without taking many-body effects into account. More experimental results are needed before one can conclude whether they are important or not.

Another approximation is that the part of the calculation where the potential $V(z)$ is calculated self-consistently is done in the axial approximation. We have seen that the classical effective masses did not change very much when we included the exact matrix (2), and we expect that $V(z)$ is not strongly dependent on the $k_{||}$ dispersion. More serious, perhaps, is that the Landau levels are calculated in the axial approximation, with implications that have been mentioned above, and that the potential $V(z)$ for $B=0$ was kept fixed. The B dependence of $V(z)$ may be important at large magnetic fields. We have also neglected effects of Landau-level broadening.

The splitoff band has not been explicitly included in the Hamiltonian matrix and the terms linear in k have also been neglected, but we do not believe that this is a serious error. The valence-band parameters are somewhat uncertain, however. In Ref. 13 the parameters determined by

Skolnick *et al.*[40] $\gamma_1=6.98$, $\gamma_2=2.25$, and $\gamma_3=2.88$ for GaAs were used. These values do not differ very much from the values that we have used (Table I), but we have found that the cyclotron effective masses for the 2D hole gas were about 10% smaller when we used the γ's determined by Skolnick *et al.*[40]

We have assumed that both the layers are semi-infinite. In the design of transistors, etc., it is desirable that the doped layer is depleted. Thus the band bending on the other side of this layer should start near the same position as the band bending at the GaAs side. This is a complication if one tries to deduce ΔE_v from the design parameters.[37] We have also found that even for the highest N_d value considered (10^{15} cm^{-3}) the width of the depletion layer in the GaAs, l_n, would be larger than the width of the GaAs layer used in Ref. 3, 1 μm. At the opposite side of this layer the Fermi level should approach a deep level in the band gap of the Cr-doped semi-insulating GaAs substrate.

We have used a generalization of the commonly applied boundary conditions for heterostructures that the envelope wave function F and $(1/m^*)(dF/dz)$ are continuous. This is a reasonable assumption since it leads to a conserved current density. The boundary conditions for the envelope function are derived using assumptions about the Bloch functions, which should be examined in more detail. Finally, there are of course numerical errors in connection with the finite basis set and the numerical integrations, but we do not believe that they are significant. As a check we have modified our program to calculate the energy levels of a 2D electron gas and found that they agree very well with the Hartree-approximation results by Stern and Das Sarma.[20]

We have assumed that the GaAs is slightly n type. If it is p type we have an accumulation layer rather than an inversion layer. The main difference is that the Fermi level then approaches the valence-band edge instead of the conduction-band edge in the bulk GaAs and the charge density due to ionized impurities is thus changed. Calculations for an accumulation layer will be presented elsewhere.

We have briefly mentioned that Bangert and Landwehr[13] and Broido and Sham[14] recently have done quite similar calculations. There are some differences in the details of the calculations but the results differ in some cases significantly. Broido and Sham,[14] for example use basis functions which go to zero at the interface, i.e., they take ΔE_v to be infinite. To compare with these results we have also done calculations for $\Delta E_v=2$ eV, i.e., a value which for practical purposes can be considered as infinite. We then find that the results practically coincide for $k=0$ but that their subbands have more dispersion, which explains their low effective masses. They have used a much smaller basis set, which probably becomes less accurate as k increases. Bangert and Landwehr[13] use a basis set which probably gives an accuracy comparable to that of our calculations. A direct comparison is complicated by the fact that they have included the image potential in their calculation for an infinite value of ΔE_v. However, if we compare the subband dispersion relative to the Fermi energy the results agree quite well. They have also done calculations for a finite ΔE_v value but concluded that the effective masses do not depend very much on ΔE_v. However, we have found that in particular the smaller effective mass strongly depends on ΔE_v. A difference in the treatment of the boundary conditions could possibly explain the discrepancy.

In any case, it is clear that none of these three calculations for $B=0$ gives two effective masses in the neighborhood of the experimental values, which are obtained at fairly high magnetic fields. The effective mass clearly depends on B as described in Sec. III. After the inclusion of a magnetic field, Bangert and Landwehr[13] found quite good agreement for the lower mass 0.38 but no transitions corresponding to $m^*\simeq 0.6$. If we compare their results to ours we find that the transition for which we found good agreement with the higher mass is the same as that for which they found $m^*\simeq 0.38$. Thus, they find a larger energy separation between these two Landau levels than we do. One possible explanation for this difference is their neglect of the background charge density in the GaAs. This implies that the slope of $V_n^{\rm dep}$ goes to zero and then the 2D hole gas becomes bound only by $V^{\rm inv}$. [See Fig. 1(b).] The strong anticrossing behavior seen in Fig. 5 is much less pronounced in Ref. 13. The cyclotron effective masses obtained by Broido and Sham[14] are only partly in agreement with experiment, and like Bangert and Landwehr they do not reproduce the larger effective mass 0.6. The reason is probably the same as was mentioned above for $B=0$, the smallness of their basis set.

The method used in this paper is also applicable to many other heterostructures. However, it cannot immediately be applied to the so-called type-II heterostructures which can be exemplified by the InAs-GaSb interface. This system is interesting because the GaSb valence-band edge lies higher in energy than the InAs conduction-band edge and a transfer of electrons from the GaSb to the InAs occurs even in the absence of doping.[45] This situation is schematically shown in Fig. 9. We see that bound electron or hole states on one side of the interface are degenerate with continuum states on the other side. Preliminary calculations suggest that the interaction between

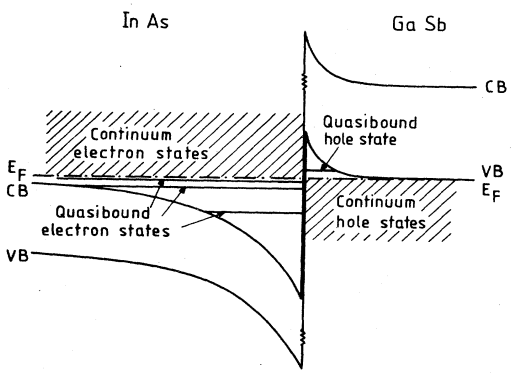

FIG. 9. Schematic band diagram for the conduction and valence bands and quasibound states at the InAs-GaSb interface. The hatched areas above the potential well for electrons in the InAs and below the potential well for holes in the GaSb indicate continuum states.

these two types of states may be important but it cannot be properly taken into account using the present formalism. This effect does not occur in the InAs-GaSb superlattice.[22] It is interesting that the quantized Hall effect has been observed[46] for the single InAs well, since it appears that the parallel conduction of electrons and holes in InAs and GaSb, respectively, would destroy this effect.

We have noted that the effective masses, both for $B=0$ and $B\neq 0$, are quite sensitive to the details of the calculation. For a better comparison with experiment, other experiments than cyclotron resonance would be desirable. The p-channel Si inversion layer has recently been examined using inelastic light scattering by Baumgartner *et al.*[47] and using parallel excitation by Wieck *et al.*,[48] and the former method has also been applied by Pinczuk *et al.*[49] for multiple GaAs wells between p-type $Al_xGa_{1-x}As$ layers. Such experiments for the present system could give information about more than the ground subband and thus be a good test of the different calculations.

V. CONCLUSIONS

We have calculated the subbands for $B=0$ and the Landau levels for $B\neq 0$ for a 2D hole gas in the envelope function approximation. The finite value of the valence-band discontinuity and the matching of the wave function at the interface have been taken into account. The potential has been calculated self-consistently in the Hartree approximation. We have found that, although the $E(k_{||})$ dispersion is found to be anisotropic, the subbands and the classical cyclotron effective masses in the axial approximation are not far from those using the exact valence-band structure [Eq. (2)]. We have also found that the axial approximation is considerably more accurate than the spherical approximation, which was used in an earlier paper.[9] When a magnetic field is included it would be cumbersome to go beyond the axial approximation.

We have found that the cyclotron effective masses strongly depend on the magnetic field and that the trends for this dependence are different for different effective masses. Thus one cannot expect to obtain good agreement between the calculated classical cyclotron effective masses (for $B=0$) and the effective masses measured in a strong magnetic field. In contrast to other calculations[13,14] we have found very good agreement with the higher experimentally determined effective mass 0.60. For the smaller mass 0.38 found in Ref. 3 we have good agreement at higher magnetic fields. Our calculation is also in agreement with the trend recently found by Eisenstein *et al.*[5] that this mass decreases with decreasing magnetic field. We have found that the results are quite sensitive to the valence-band discontinuity ΔE_v and the background impurity concentration in the GaAs and have shown how the effective masses change with the areal hole density N_s. We have also given explanations for the discrepancies among our calculation, that by Bangert and Landwehr,[13] and that by Broido and Sham.[14] For a better check of our results we have proposed some experiments, which also would give information about excited subbands.

Note added in proof. Accurate calculations of subbands and classical cyclotron effective masses have very recently been published [T. Ando, J. Phys. Soc. Jpn. **54**, 1528 (1985)]. These results agree very well with ours.

ACKNOWLEDGMENTS

We gratefully acknowledge stimulating discussions with Dr. E. Bangert and Dr. J. C. Maan. We are also thankful to D. A. Broido and Dr. K. Ploog for communicating results prior to publication and to Dr. P. Horsch for a critical reading of the manuscript.

[1]H. L. Störmer and W.-T. Tsang, Appl. Phys. Lett. **36**, 685 (1980).
[2]H. L. Störmer, A. Chang, D. C. Tsui, J. C. M. Hwang, A. C. Gossard, and W. Wiegmann, Phys. Rev. Lett. **50**, 1953 (1983).
[3]H. L. Störmer, Z. Schlesinger, A. Chang, D. C. Tsui, A. C. Gossard, and W. Wiegmann, Phys. Rev. Lett. **51**, 126 (1983).
[4]H. L. Störmer, A. C. Gossard, W. Wiegmann, R. Blondel, and K. Baldwin, Appl. Phys. Lett. **44**, 139 (1984).
[5]J. P. Eisenstein, H. L. Störmer, V. Narayanamurti, A. C. Gossard, and W. Wiegmann, Phys. Rev. Lett. **53**, 2579 (1984).
[6]H. L. Störmer, K. Baldwin, A. C. Gossard, and W. Wiegmann, Appl. Phys. Lett. **44**, 1062 (1984).
[7]S. Tiwari and W. I. Wang, IEEE Electron Dev. Lett. **EDL-5**, 333 (1984).
[8]R. A. Kiehl and A. C. Gossard, IEEE Electron Dev. Lett. **EDL-5**, 521 (1984).
[9]U. Ekenberg and M. Altarelli, Phys. Rev. B **30**, 3569 (1984).
[10]J. M. Luttinger, Phys. Rev. **102**, 1030 (1956).
[11]J. M. Luttinger and W. Kohn, Phys. Rev. **97**, 869 (1955).
[12]A. Baldereschi and N. O. Lipari, Phys. Rev. B **8**, 2697 (1973).
[13]E. Bangert and G. Landwehr, in Proceedings of the International Conference on Superlattices, Microstructures and Microdevices, Urbana-Champaign, Illinois, 1984 [Superlattices Microstr. Microdev. (to be published)].
[14]D. A. Broido and L. J. Sham, Phys. Rev. B **31**, 888 (1985).
[15]D. E. Aspnes and A. A. Studna, Phys. Rev. B **7**, 4605 (1973).
[16]G. Dresselhaus, Phys. Rev. **100**, 580 (1955).
[17]N. O. Lipari and M. Altarelli, Phys. Rev. B **15**, 4883 (1977).
[18]F. J. Ohkawa, J. Phys. Soc. Jpn. **41**, 122 (1976).
[19]Gaussian units are used throughout the paper.
[20]F. Stern and S. Das Sarma, Phys. Rev. B **30**, 840 (1984).
[21]H. Schlosser and P. M. Marcus, Phys. Rev. **131**, 2529 (1963), especially Appendix 1.
[22]M. Altarelli, Phys. Rev. B **28**, 842 (1983).
[23]A. Fasolino and M. Altarelli, in *Two-Dimensional Systems, Heterostructures and Superlattices,* edited by G. Bauer, F. Kuchar, and H. Heinrich (Springer, Berlin, 1984), p. 176.
[24]K. Suzuki and J. C. Hensel, Phys. Rev. B **9**, 4184 (1974).
[25]H.-R. Trebin, U. Rössler, and R. Ranvaud, Phys. Rev. B **20**, 686 (1979).
[26]K. Hess, D. Bimberg, N. O. Lipari, J. U. Fischbach, and M. Altarelli, in *Proceedings of the 13th International Conference on the Physics of Semiconductors,* edited by F. G. Fumi (Marves, Rome, 1976), p. 142.
[27]E. Hess, I. Topol, K.-R. Schulze, H. Neumann, and K. Unger, Phys. Status Solidi B **55**, 187 (1973).
[28]P. Lawaetz, Phys. Rev. B **4**, 3460 (1971).
[29]G. E. Stillman, D. M. Larsen, C. M. Wolfe, and R. C. Brandt, Solid State Commun. **9**, 2245 (1971).
[30]H. C. Casey, Jr. and M. B. Panish, *Heterostructure Lasers:*

Part A, Fundamental Principles (Academic, New York, 1978).
[31]R. Dingle, A. C. Gossard, and W. Wiegmann, Phys. Rev. Lett. **34**, 1327 (1975).
[32]R. People, K. W. Wecht, K. Alavi, and A. Y. Cho, Appl. Phys. Lett. **43**, 118 (1983).
[33]R. C. Miller, D. A. Kleinman, and A. C. Gossard, Phys. Rev. B **29**, 7085 (1984).
[34]D. Arnold, A. Ketterson, T. Henderson, J. Klem, and H. Morkoç, Appl. Phys. Lett. **45**, 1237 (1984).
[35]J. Batey, S. L. Wright, and D. J. DiMaria, J. Appl. Phys. **57**, 484 (1985).
[36]Y. Horikoshi, A. Fischer, and K. Ploog, Phys. Rev. B **31**, 7859 (1985). The same value has also been found by U. Prechtel, G. Abstreiter, and G. Weimann (unpublished).
[37]W. I. Wang, E. E. Mendez, and F. Stern, Appl. Phys. Lett. **45**, 639 (1984). See also F. Stern, Appl. Phys. Lett. **43**, 974 (1983).
[38]H. Okamura, S. Misawa, S. Yoshida, and S. Gonda, Appl. Phys. Lett. **46**, 377 (1985).
[39]The calculations in Ref. 9 were affected by a numerical error. The resulting error in the subband energies was, however, small compared to the difference between the results in the spherical and the axial approximations.
[40]M. S. Skolnick, A. K. Jain, R. A. Stradling, J. Leotin, J. C. Ousset, and S. Askenazy, J. Phys. C **9**, 2809 (1976).
[41]We are grateful to Dr. E. Bangert for drawing our attention to this possibility.
[42]See, e.g., T. Ando, Phys. Rev. B **13**, 3468 (1976).
[43]T. Ando, J. Phys. Soc. Jpn. **51**, 3893 (1982).
[44]G. Landwehr, E. Bangert, K. von Klitzing, Th. Englert, and G. Dorda, Solid State Commun. **19**, 1031 (1976).
[45]Y. Guldner, J. P. Vieren, P. Voisin, M. Voos, J. C. Maan, L. L. Chang, and L. Esaki, Solid State Commun. **41**, 755 (1982).
[46]E. E. Mendez, L. L. Chang, C.-A. Chang, L. F. Alexander, and L. Esaki, Surf. Sci. **142**, 215 (1984).
[47]M. Baumgartner, G. Abstreiter, and E. Bangert, J. Phys. C **17**, 1617 (1984).
[48]A. D. Wieck, E. Batke, D. Heitmann, J. P. Kotthaus, and E. Bangert, Phys. Rev. Lett. **53**, 493 (1984).
[49]A. Pinczuk, H. L. Störmer, A. C. Gossard, and W. Wiegmann, in *Proceedings of the 17th International Conference on the Physics of Semiconductors, San Francisco, 1984,* edited by J. D. Chadi and W. A. Harrison (Springer, New York, 1985). p. 329.